Aging Brain 7 (2025) 100134

Contents lists available at ScienceDirect

Aging Brain

journal homepage: www.elsevier.com/locate/nbas

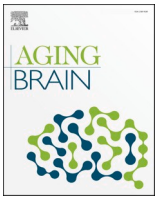

TOMM40 may mediate GFAP, neurofilament light Protein, pTau181, and brain morphometry in aging

Robyn A. Honea [a,b,*], Heather Wilkins [a,b,c], Suzanne L. Hunt [a,d], Paul J. Kueck [a,b], Jeffrey M. Burns [a,b], Russell H. Swerdlow [a,b,c,e], Jill K. Morris [a,b,c]

[a] University of Kansas Alzheimer's Disease Research Center, University of Kansas Medical Center, Kansas City, KS, 66160, USA
[b] Department of Neurology, University of Kansas School of Medicine, Kansas City, KS, 66160, USA
[c] Department of Biochemistry and Molecular Biology, University of Kansas Medical Center, Kansas City, KS, 66160, USA
[d] Department of Biostatistics and Data Science, University of Kansas Medical Center, Kansas City, KS, 66160, USA
[e] Department of Cell Biology and Physiology, University of Kansas Medical Center, Kansas City, KS, 66160, USA

ARTICLE INFO

Keywords:
TOMM40
APOE
NfL
pTau181
Aging
GFAP
Alzheimer's Disease
Gray matter volume
Neuroimage
Mitochondria

ABSTRACT

A growing amount of data has implicated the *TOMM40* gene in the risk for Alzheimer's disease (AD), neurodegeneration, and accelerated aging. No studies have investigated the relationship of *TOMM40* rs2075650 ('650*)* on the structural complexity of the brain or plasma markers of neurodegeneration. We used a comprehensive approach to quantify the impact of *TOMM40* '650 on brain morphology and multiple cortical attributes in cognitively unimpaired (CU) individuals. We also tested whether the presence of the risk allele, G, of *TOMM40* '650 was associated with plasma markers of amyloid, tau, and neurodegeneration and if there were interactions with age and sex, controlling for the effects of *APOE* ε4. We found that the *TOMM40* '650 G-allele was associated with decreased sulcal depth, increased gyrification index, and decreased gray matter volume. NfL, GFAP, and pTau181 had independent and age-associated increases in individuals with a G-allele. Our data suggest that *TOMM40* '650 is associated with aging-related plasma biomarkers and brain structure variation in temporal-limbic circuits.

1. Introduction

A complex interplay of genes impacts the underlying biological mechanisms of aging. The locus on chromosome 19 containing *TOMM40*, *APOE*, and *APOC1* has been identified as a critical hub for human longevity [14,18,61]. *TOMM40*, or Translocase of the Mitochondrial Membrane 40, is a close neighbor to and in linkage disequilibrium with *APOE* [41]. Sequence variants in both *TOMM40* and *APOE* have been associated with cognitive aging, longevity, aging-related brain structure and function biomarkers, and possible genetic contribution to the "mitochondrial cascade hypothesis." *TOMM40* may have both independent and interactive (i.e., with *APOE*) effects on aging and especially risk for Alzheimer's disease (AD)[33,50], although its multifaceted role is still being investigated. The mitochondrial cascade hypothesis suggests that multiple interacting factors impact baseline and age-related decline in mitochondrial function [60]. *TOMM40* is the primary nuclear encoded AD-risk gene impacting AD-related mitochondrial dysfunction [20]. *TOMM40's* mechanism contributing to the risk for AD is most likely a complex disruption of cellular bioenergetics in the

* Corresponding author at: KU Alzheimer's Disease Research Center, University of Kansas Medical Center, 4350 Shawnee Mission Parkway, MS 6002, Fairway, KS 66205, USA.
E-mail address: rhonea@kumc.edu (R.A. Honea).

https://doi.org/10.1016/j.nbas.2024.100134
Received 24 April 2024; Received in revised form 9 December 2024; Accepted 11 December 2024
Available online 13 December 2024

mitochondria. Still, the relationship between these dysfunctions and AD-related neurodegeneration is not clear.

A recent systematic review of all *TOMM40* variants associated with healthy aging and longevity identified the *TOMM40* single-nucleotide polymorphism (SNP) rs2075650 ('650) as the most identified SNP in *TOMM40* associated with longevity [11]. *TOMM40*'650 is located within the noncoding region of *TOMM40*: c.275-31A > G. The minor allele frequency for G in European populations is roughly 0.130 ((Allele Frequency Aggregator 2023 (ALFA) https://www.ncbi.nlm.nih.gov/snp/rs2075650#frequency_tab). The A allele of *TOMM40*'650 has been consistently linked to increased longevity across several populations including Chinese, United States and Europe[14,38,39,53,70,71]with one study noting increased longevity in women [54]. On the other hand, the G-allele has been associated with several interesting features, including lower BMI in aging, delayed verbal recall, and decreased language comprehension, with possible differences between sexes [1,32,35]. There have also been several studies showing that a G versus an A allele on *TOMM40* '650 increases the risk for accelerated aging and Alzheimer's disease [33,49]. Individuals with a G-allele may also have increased inflammatory markers [34], vascular risk factors, and cognitive decline [22].

Despite the role *TOMM40* '650 appears to have on aging and aging-related disease, its relationship with neurodegeneration and typical plasma biomarkers of AD is unestablished. Neurofilament light (NfL) proteins are a marker of neuronal damage and can be measured in CSF and plasma. Glial fibrillary acidic protein (GFAP) also plays a role in aging, particularly in the brain, and GFAP expression is increased with aging. APOE, TOMM40 '650, and APOC1 risk combinations may also influence Aβ and Tau in CSF [31]. However, the specific genetic impact of *TOMM40* on aging-related biomarkers is unclear. Given the role of *TOMM40* '650 in aging, longevity, and inflammation, we sought to evaluate its association with plasma markers of ATN (amyloid (Aβ42, and Aβ40), tau (P-tau181) and neurodegeneration (GFAP and NfL).

Specific features of structural MRI may provide more sensitive phenotypes to intricate genetic effects in the brain. For instance, the quantification of local fractal dimension (FD) using spherical harmonic reconstructions yields more detailed insights into the complexity of cortical folding [72,73]. Fractal dimension analysis has revealed significant differences in the structural complexity of gray matter, which tends to decrease with aging and is altered in neurological diseases [30,37,42]. Additionally, studies have identified specific regional patterns of cortical thinning associated with Alzheimer's disease[13,16], which are evident even in the early stages of cognitive decline [29]. The gyrification index quantitatively measures cortical folding by calculating the ratio of the total pial surface area to the superficial cortical surface area, offering insights into cortical changes during atrophy. Sulcal depth, which measures the Euclidean distance between the pial and outer surfaces, has also been potentially sensitive in detecting mild cognitive impairment (MCI)[7427]. No previous study has investigated the relationship *TOMM40* '650 on the structural complexity of the brain using fractal dimension, gyrification index, or sulcal depth, for which there may be subtle differences in mitochondrial-related gene changes. We aimed to use whole brain voxel-based (VBM) and surface-based morphology (SBM) methods to test whether *TOMM40* genetic variation differentially impacted brain volume, cortical thickness, sulcal depth, fractal dimension, and gyrification index measures. Based on structural imaging studies on *APOE* ε4 and *TOMM40* to date, we hypothesized that the presence of a '650 G-allele would be related to reduced volume, thinner cortex, shallower sulcal depth, reduced fractal dimension, and lower gyrification index in AD-related temporal and parietal regions compared to *TOMM40* A/A-carriers. Specifically, we hypothesized that we would see morphometric differences in the hippocampus, parahippocampus, superior temporal, and precuneus cortices. We also hypothesized that otherwise healthy individuals with a '650 G-allele would have plasma ATN markers (NfL, pTau181, GFAP, Aβ42, and Aβ40) indicative of possible risk for AD.

2. Materials and methods

2.1. Standard protocol Approvals, Registrations, and Patient Consents

Study procedures were approved by the University of Kansas School of Medicine Institutional Review Board and were in accordance with U.S. federal regulations. All participants provided written informed consent.

2.2. Participants

Participants were recruited as part of the intervention and observational studies at the University of Kansas Alzheimer's Disease Research Center (KU ADRC) and were part of the Clinical Cohort. The KU ADRC is part of the U.S. network of Alzheimer's Disease Centers of Excellence that supports research into brain aging and dementia. Beginning in 2004, we developed a registry of individuals who have consented to be contacted regarding research studies, details of which have been published elsewhere[64]. The KU ADRC collects longitudinal data on a clinical cohort of over 400 individuals. The cohort includes participants with cognitive impairment as well as healthy cognition. Cognitively unimpaired individuals (CU) were included at age 60 and older. The Uniform Data Set (UDS) was created in 2005 to collect standard clinical data on participants from the National Institute on Aging (NIA)-supported Alzheimer's Disease Centers (ADCs). The UDS is administered to ADC Clinical Cohort participants approximately annually. Individuals were included in this retrospective analysis if they underwent brain imaging and *TOMM40 '650* genotyping as part of these ongoing observational and intervention-based studies (pre-intervention timepoint only) on fitness, exercise, aging, and risk for AD, and the total that had this type of data was 113 (ClinicalTrials.gov: NCT01129115, NCT02000583, NCT00267124).

All participants also underwent a standard examination, which includes a thorough clinical and cognitive evaluation with a clinician at the KU ADRC. This clinical evaluation consists of a semi-structured interview (Clinical Dementia Rating, CDR) with the participant and study partner [48]and a physical and neurological examination. Clinical evaluation results were used to verify cognitively unimpaired status (CU), which were reviewed along with psychometric battery results and finalized at a consensus

diagnostic conference attended by clinicians and psychometricians using the NINCDS-ADRDA criteria as well as the McKann NIA-AA workgroup diagnostic guidelines [7,44]. Individuals were excluded from participating if they had other neurological disorders that could impair cognition, evidence of bleeding disorders during screening, clinically significant disease, psychiatric disorder, systemic illness, stroke, or myocardial infarction.

A psychometrician administered a standard psychometric battery as described in a previous publication [66]. As published previously, we used Mplus to combine test scores into cognitive domain-specific factor scores using confirmatory factor analysis, and specific tests were organized by whether they measured attention, verbal memory, or executive function [65]. Domain-specific factor scores were used as descriptive variables in our demographics analysis. Other covariates included the Geriatric Depression Scale (GDS), the Montreal Cognitive Assessment (MoCA), and Mini-Mental State Examination (MMSE). Participants completed thorough family history examinations using a standard family history questionnaire, as described elsewhere [26,68].

2.3. Genotyping and plasma marker procedures

Determination of *APOE* genotype was performed by the National Cell Repository for Alzheimer's Disease (NCRAD), with independent verification of selected samples by the KU ADRC Biomarker Core using a previously described allelic discrimination assay [67]. For the *APOE* genotype, participants were categorized as having ε2, ε3, or ε4 genotypes, which we used as a covariate in place of the number of *APOE* alleles, which may help disentangle relationships between *APOE* ε4 and *TOMM40* '650 [35]. APOE 2/2 was defined as homozygous TT for both rs429358 and rs7412 SNPs. APOE 2/3 was defined as homozygous TT for rs429358 SNP and heterozygous CT for rs7412 SNP. APOE 2/4 was defined as heterozygous CT for both rs429358 and rs7412 SNPs. APOE 3/3 was defined as homozygous TT for rs429358 SNP and homozygous CC for rs7412 SNP. APOE 3/4 was defined as heterozygous CT for rs429358 SNP and homozygous CC for rs7412 SNP. APOE 4/4 was defined as homozygous CC for both rs429358 and rs7412 SNPs. Linkage disequilibrium (LD)was also tested between rs2075650 and the *APOE* SNPs rs429358 and rs7412, with the LD map shown in Fig. 1. The KU ADRC Biomarker Core performed *TOMM40* rs2075650 genotyping. Genotyping was performed from whole blood samples. Genomic DNA was isolated with Qiagen kits and then PCR amplified using TaKaRa Ex Taq polymerase with 5 % DMSO and the following primers (0.4 μM each): forward FAM-TGCTGACCTCAAGCTGTCCTC and reverse GAGGCTGAGAAGGGAGGATT. PCR products were purified using ExoSAP-IT (ThermoFisher) and sent to Genewiz (Azenta) for fragment analysis.

Additional blood was collected using EDTA as an anticoagulant and centrifuged at 1800 x g to generate plasma. Samples were frozen at −80C before analyses. Markers of ATN were measured for Plasma NfL, pTau181, GFAP, Aβ42, and Aβ40 using a Simoa HD-X (Quanterix, Billerica, MA). Kits were run for pTau181 (v2.0) and neuro four plex E (N4PE) according to manufacturer instructions with appropriate standards and quality control samples [21]. All samples were run in duplicate, and the mean concentration of the blood biomarkers was recorded from each blood sample. Additionally, the ratio of Aβ42 to Aβ40 was calculated for each sample (Aβ42/40).

2.4. Structural brain imaging Acquisition

All participants coming through neuroimaging studies at the KU ADRC underwent magnetic resonance imaging (MRI) of the brain in either a Siemens 3.0 Tesla Allegra or Skyra scanner. We obtained a high-resolution T1-weighted image (MP-RAGE; 1 × 1 × 1 mm voxels; TR = 2500 ms, TE = 4.38 ms, TI = 1100, FOV = 256X256 with 18 % oversample, 1 mm slice thickness, flip angle 8 deg) for

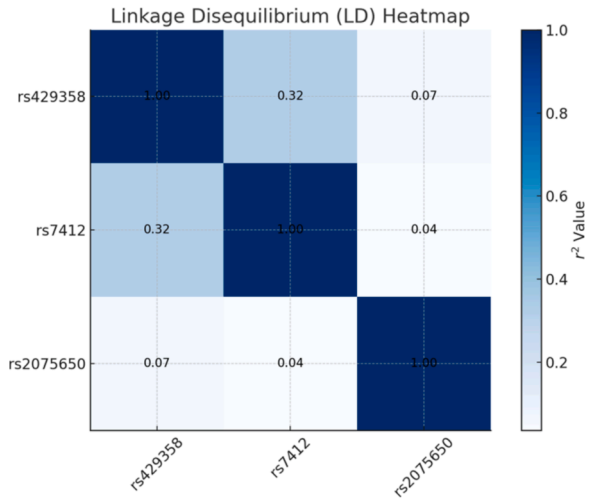

Fig. 1. Linkage Disequilibrium (LD) pattern for rs2075650, rs429358, and rs7412 SNPs in the study sample. The numbers in the boxes are the pairwise correlation coefficient r^2 between respective SNPs. r^2 values of 1 represent complete LD, r^2 values greater than 0.8 represent strong LD, r^2 values of 0.2–0.8 represent inconclusive LD, and r^2 less than 0.2 represent negligible evidence of LD. There was negligible LD between *TOMM40* rs2075650 and the two *APOE* SNPs rs4712 and rs429358 in this sample.

detailed anatomy with high gray-white matter contrast. We did cortical surface-based (estimation of cortical thickness, the complexity of cortical folding based on fractal dimension (FD), gyrification index, and sulcal depth) analyses along with VBM and region of interest analyses. Every scan was checked for image artifacts and gross anatomical abnormalities. 113 CU individuals with MPRAGE scans and participating in the genetics protocol passed quality control.

2.5. Voxel-Based and Surface-Based morphometry

For VBM and SBM analysis and pre-processing of T1-weighted images, we used the Computational Anatomical Toolbox 12 (CAT12 Version 12.6, C. Gaser, Structural Brain Mapping Group, Jena University Hospital, Jena, Germany; https://dbm.neuro.uni-jena.de/cat/) through Statistical Parametric Mapping version 12 (SPM12; Wellcome Trust Centre for Neuroimaging, London, UK; https://www.fil.ion.ucl.ac.uk/spm/software/spm12/)) that operate under Matlab (R2019b) (the Mathworks, Natick, MA) on Mac. This was used for brain volume (VBM) and surface-based measures such as cortical thickness (CT), sulcal density (SD), GI (gyrification index), and fractal dimension (FD). All the SBM procedures (https://www.neuro.uni-jena.de/cat12/CAT12-Manual.pdf) were conducted using default settings.

T1 images were corrected for bias-field inhomogeneities, registered using linear (12-parameter affine) and non-linear transformations, spatially normalized using the high-dimensional DARTEL algorithm into MNI space [3]and segmented into gray matter (GM), white matter (WM), cerebrospinal fluid (CSF) and white matter hyperintensity (WMH). We calculated total intracranial volume (TIV) using gray, white, and CSF volumes. The volume changes were scaled in order to retain the original local volumes (modulating the segmentations) [19]. The modulated gray matter segmentations were smoothed using a $10 \times 10 \times 10$ mm full-width at half-maximum Gaussian kernel before group level voxel-wise analysis. Resampled surface data for cortical thickness (CT), fractal dimension (FD), and sulcal depth (SD) were smoothed using a 15 mm FWHM kernel, and data for gyrification were smoothed using a 25 mm FWHM kernel prior to 2nd level analyses.

2.5.1. VBM and SBM- statistical analysis

For all analyses, voxels are reported with reference to the MNI standard space within SPM12. To avoid possible edge effects at the border between GM and WM and to include only relatively homogeneous voxels, we used an absolute threshold masking of 0.10 for each analysis. In order to investigate associations between *TOMM40*'650 groups and gray matter volume differences, we included age, sex, education, *APOE* ε4 carrier status, and total intracranial volume (TIV) as variables of no interest in our full factorial model. Statistics were done in imaging space across all voxels. A full-factorial analysis was done comparing 1) *TOMM40*'650 AA and G-Carrier groups, including age, sex, education, and *APOE* haplotype (ε2, ε3, and ε4 groups) and 2) *TOMM40*'650 AA ε4 negative individuals compared with *TOMM40*'650 G-Carrier ε4 negative, including age, sex and education as covariates. Significance was determined via the threshold-free cluster enhancement method (TFCE) [58], which allows for cluster-based inference without the need to pre-specify arbitrary thresholds. This implementation in the TFCE toolbox for CAT12 performs parametric permutation tests, thus avoiding problems inherent to parametric statistics [17], and has been recommended in similar SBM-based whole-brain analyses [5]. Family-wise error (FWE) correction was applied to the entire brain, and we considered a corrected $p < 0.05$ as significant. Anatomical labeling from the Wakeforest Pickatlas AAL atlas was used to identify peak coordinate regions in VBM and SBM. The Desikan-Killiany [15]atlas was used for SBM (and AAL for VBM) to extract mean regional values from the processed images in significant regions after voxel-wise analysis.

Table 1
Demographic Characteristics of sample.

***TOMM40* '650**	**A/A**	**G-Carrier**	**p-value**
N = 113	**83**	**30**	
Years of Age (SD)	74.8 (6.4)	72.9 (5.9)	0.164
Education (years)	16.94 (2.8)	16.3 (3.4)	0.324
Gender (M/F)	38/45	11/19	0.259
GDS Score	1.07 (1.77)	0.86 (1.1)	0.548
MoCA	25.6 (4.3)	26.1 (2.8)	0.55
Verbal memory factor	−0.547 (0.93)	−0.724 (0.86)	0.264
Attention factor	−0.251 (0.41)	−0.310 (0.45)	0.982
Executive factor	−0.375 (0.56)	−0.484 (0.49)	0.592
Total Intracranial Volume (mm^3)	1398.9 (153)	1349 (133)	0.28
Gray Matter Volume, TIV adjusted	0.401 (0.03)	0.407 (0.02)	0.926
White Matter Volume, TIV adjusted	0.339 (0.02)	0.341 (0.02)	0.685
White Matter Hyperintensity Volume (mm^3)	4.68 (6.7)	4.24 (4.3)	0.496
FH (−/FHm/FHp/FHboth) (N = 57)	18/9/8/5	2/9/2/4	**0.035**
FH (−/+) (N = 57)	18/22	2/15	**0.016**
APOE ε4 Carrier (Negative/Positive)	68/15	8/22	**0<.001**

Demographic, neuropsychological, and MRI characteristics of the CU individuals from the VBM and SBM analysis. Values are mean (SD (standard deviation)) except for sex and age range. Covariates included age, sex, and education for univariate analysis. FH; family history of dementia, FH+; positive family history of dementia, FH-; negative family history of dementia, FHm; maternal family history of dementia, FHp; paternal family history of dementia; FHBoth; both parents with a family history of dementia, M; male, F; female, TIV; Total Intracranial Volume, mm; millimeter, MMSE; Mini-Mental Status Exam, GDS; Geriatric Depression Score, MoCA; Montreal Cognitive Assessment, N; number. Significant values in bold.

2.6. Statistical analyses

SPSS 23.0 (IBM Corp., Armonk, NY) was used for the statistical analyses performed outside of imaging space. Continuous demographic, cognitive, plasma markers, and volumetric imaging variables (dependent variables) were compared between *TOMM40* '650 AA and G-Carrier groups using the one-way multivariate analysis of covariance (MANCOVA) for the descriptive statistics. A chi-square analysis was used to compare categorical demographic variables between groups. We included participants' age, sex, and *APOE* haplotype (ε2, ε3, and ε4 groups) as covariates in the MANCOVA when testing cognitive domain scores, plasma variables and brain volumes. We then tested for interactions of age and sex between *TOMM40 '650* groups and the mean blood plasma pTau181, GFAP, NfL, and Aβ 42/40, covarying for *APOE* haplotype. Raw p-values < 0.05 were nominally significant. In a post-hoc analysis, based on the results of the voxel and surface-based morphometry, we used ANCOVA between the *TOMM40* '650 groups to test for interactions of age and sex between the mean gray matter volume in regions already found to be significant in the VBM and SBM analyses, covarying for *APOE* haplotype.

3. Results

3.1. Demographics and plasma markers

Demographic and neuropsychological data are presented in Table 1. Genotype groups were not significantly different in mean age, education, sex, MoCA, cognitive factor scores, global brain volumes, or geriatric depression scale scores (GDS) (Table 1). There was a significant difference between family history positivity between the groups in a subgroup of our sample that had complete FH data, with the G-allele carriers having a higher proportion of FH+ (particularly FHm) than A homozygotes. As expected, there was a larger proportion of *APOE* ε4 carriers in the G-allele carriers ($p < 0.001$). Mean and range differences in plasma biomarkers are shown in Table 2. The main effect of '650 G-allele carriage was associated with GFAP, pTau181,and NfL, and interactions with age and '650 were observed (Table 3, Fig. 2). There were no significant effects of '650 G-allele carriage or interactions with age or sex with Aβ 42/40 ratio. There were no significant three-way interactions with sex or age and sex in plasma markers.

3.2. Voxel and Surface-Based morphometry between TOMM40 '650 genotype groups

In the voxel-based analysis of gray matter volume across'650 genotype groups, including age, sex, education, and *APOE* ε4 Haplogroup in the model as covariates, we found that individuals with a G-allele had significantly decreased volume in the medial temporal complex, specifically the left middle temporal gyrus, right fusiform gyrus, the right inferior temporal gyrus. G-carriers also had significantly reduced gray matter volume in the left inferior parietal cortex, right cuneus, and the right superior and middle frontal gyri (Table 4). When looking only at *APOE* ε4 negative *'650* genotype groups, we also found significantly lower gray matter volume in the G-allele carrying individuals in the left inferior temporal, right middle temporal, right parahippocampal, right cuneus and left and right superior frontal gyrus (Table 4, Fig. 3). There were no significant differences between '650 genotype groups in the inverse statistical contrasts across gray matter volume measures.

In the surface-based analysis of gray matter volume across'650 genotype groups, including age, sex, education, and *APOE* ε4 Haplogroup in the model as covariates, we found no significant differences across morphological measures. When looking only at *APOE* ε4 negative *'650* genotype groups we found that individuals with a G-allele had significantly increased sulcal depth in the right superior temporal gyrus, right medial superior frontal gyrus, right postcentral gyrus and left lingual gyrus (Table 4, Fig. 3. We also found significantly smaller gyrification index in the ε4-negative G-allele-carrying individuals in the left inferior parietal and superior parietal cortices, bilateral precentral gyrus and the right postcentral gyrus (Table 4, Fig. 3). There were no significant differences between '650 genotype groups in the cortical thickness and fractal dimension analyses or inverse statistical contrasts across all morphometry measures.

3.3. TOMM40 '650 brain volume interactions

There were two regions in which there were significant interactions between G-carrier status and age: volume of the right middle temporal gyrus and right olfactory cortex ($p = 0.021$, $p = 0.044$). There were significant sex by G-carrier status interactions on left amygdala volume ($p = 0.026$), right middle temporal gyrus ($p = 0.011$), and right olfactory cortex ($p = 0.032$); the first two are plotted

Table 2
TOMM40 '650 groups with Plasma markers of ATN.

	N	A/A	G-Carrier
Plasma	**Total, AA / G-Carrier**	**Mean (Range)**	**Mean (Range)**
pTau181	n = 53, 40/13	2.14 (1.8–2.47)	2.69 (1.95–3.42)
GFAP	n = 58, 45/13	185. 06 (163–207)	202.9 (136–269)
NfL	n = 53, 45/13	32.51 (25.9–39.13)	24.76 (15.2–34.3)
Aβ 42	n = 60, 47/13	8.47 (6.21–10.74)	6.45 (5.47–7.42)
Aβ 40	n = 59, 46/13	123.6 (112.6–134.7)	121.4 (107.5–135.3)
Aβ 42/40	n = 59, 46/13	0.059 (0.056-0.064)	0.056 (0.048-0.063)

Table 3
Main effects and interactions of *TOMM40 '650* G-carriage on Plasma Markers of ATN.

	Sig	F	Sig	F	Sig	F	Sig	F
	650		**650 x Age**		**650 x sex**		**650 x age x sex**	
pTau181	**0.022**	**5.61**	**0.022**	**5.692**	0.848	0.037	0.176	1.812
GFAP	**0.002**	**10.74**	**0.002**	**11.21**	0.249	1.199	0.573	0.322
NfL	**0.012**	**6.813**	**0.015**	**6.386**	0.417	0.67	0.196	1.687
Aβ 42/40	0.833	0.045	0.822	0.051	0.28	1.191	0.496	0.712

Sig; Significance, Significant estimates in bold $p < 0.05$, controlling for *APOE ε4* Haplogroup, age and sex.

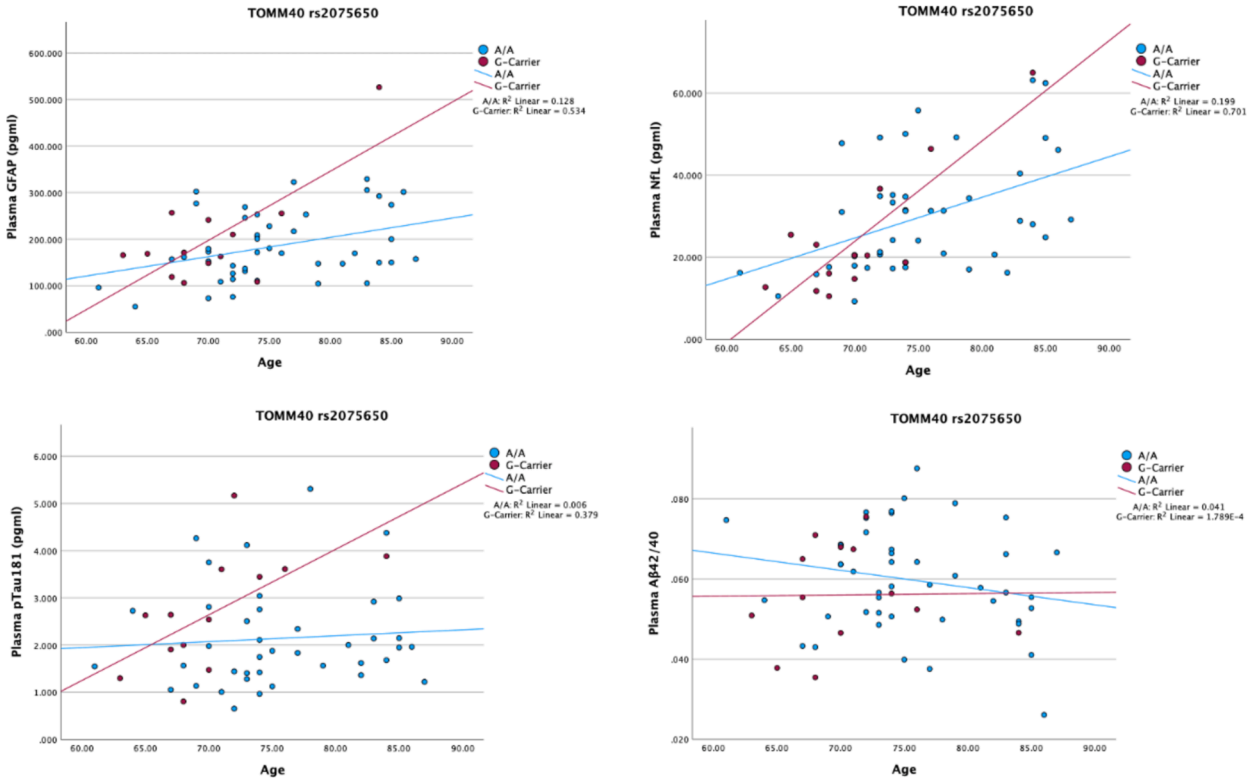

Fig. 2. Plot of TOMM40 '650 G carriage on Plasma Biomarkers. Red and blue circles represent datapoints for *TOMM40 '650* G-Carrier and AA homozygotes, respectively. There were significant interactions between G-Carrier status and age in plasma GFAP ($p = 0.002$), pTau181 ($p = 0.022$), and NfL ($p = 0.015$). The sample size for the Plasma analysis was 58 for GFAP, 59 for Aβ42/40, and 53 for NfL and pTau181.

for visual purposes in Fig. 4. There were significant 3-way interactions with sex and age in the right middle temporal gyrus ($p = 0.014$) and the left rectus gyrus ($p = 0.017$) (Table 5).

4. Discussion

In this study, we sought to characterize the relationship of *TOMM40* '650 on morphological biomarkers of cortical complexity, plasma biomarkers of AD-related pathology and neurodegeneration, and interactions of age and sex in CU individuals. We found that the *TOMM40* '650 G-allele was associated with lower gray matter volume, sulcal depth, and increased gyrification index in temporo-limbic regions of the brain. We also report that pTau181, NfL and GFAP have age-associated increases in individuals with a G-allele. Our data suggest that *TOMM40 '650* is associated with aging-related brain structure variation in temporal-limbic circuits.

Our data contribute to a growing literature supporting the role of several *TOMM40* variants on cortical complexity of the brain in limbic, temporal and precuneus cortices in the aging brain, perhaps during the preclinical phase of AD. We have recently found that healthy aging individuals with *TOMM40'523* poly-T S-alleles have more AD-related biomarkers of cortical complexity than those with *APOE ε4* and *TOMM40 VL*-alleles [25]. Varathan et al. also found a significant gene-AD association in several SNPs of *TOMM40* with cortical thickness in the temporal lobe [62]. Emergent scientific data on cognitively unimpaired individuals argues for TOMM40'523 Poly-T alleles' impact on CSF, imaging, cognitive, and mitochondrial function[12].

In this study we identified *TOMM40 '650* G-carrier specific changes in sulcal depth in the superior temporal gyrus, and in volume in

Table 4
Morphometrical differences in Volume, Sulcal Depth, and Gyrification Index between '650 TOMM40 groups.

Comparison	Size (vertexes)	TFCE	Combined Peak/Cluster p value (FWE) corrected	Coordinates (mm mm mm)	Brain Region
Volume					
AA > G Carrier	15,722	1660.41	0.018	−57 −20 −16	L Middle Temporal Gyrus
	1454	1347.31	0.037	8 −93 3	R Cuneus
	373	1341.32	0.037	−45 −54 6	L Middle Temporal Gyrus
	757	1341.05	0.037	68 −27 −22	R Inferior Temporal Gyrus
	31	1227.51	0.048	−33 −45 54	L Inferior Parietal
	203	1226.11	0.048	33 46 −9	R Middle Frontal Gyrus
	72	1224.22	0.048	−42 −88 9	L Middle Occipital Gyrus
	82	1222.79	0.049	20 66 −10	R Superior Frontal Gyrus
	73	1220.18	0.049	50 −3 −30	R Fusiform Gyrus
AA E4 Neg > G Carrier E4 Neg	1693	1656.16	0.007	56 −22 −21	R Inferior Temporal Gyrus
	617	1551.47	0.009	36 −84 15	R Middle Temporal Gyrus
	1261	1514.51	0.01	26 18 −10	R Putamen
	3677	1478.52	0.011	−48 33 0	Left Inferior Frontal Gyrus
	54	1463.77	0.012	−18 60 28	L Superior Frontal Gyrus
	186	1433.57	0.013	30 51 34	R Superior Frontal Gyrus
	63	1408.04	0.014	50 −12 24	R Postcentral Gyrus
	63	1398.7	0.014	54 −74 21	R Middle Temporal Gyrus
	286	1392.3	0.014	−3 18 3	L Caudate
	94	1384.12	0.015	2 24 14	R Anterior Cingulate
	1053	1376.41	0.015	21 8 −28	R Parahippocampal Gyrus
	523	1298.82	0.019	22 −93 8	R Cuneus
	555	1252.81	0.021	−20 −98 10	L Middle Occipital Gyrus
	151	1236.26	0.022	28 33 54	R Superior Frontal Gyrus
	61	1218.19	0.023	56 −48 −3	R Middle Temporal Gyrus
	158	1142.03	0.029	30 28 32	R Middle Frontal Gyrus
Sulcal Depth					
AA E4 Neg > G Carrier E4 Neg	5291	15918.41	0.005	65 −37 10	R Superior Temporal Gyrus
	7515	12460.16	0.013	12 46 −1	R Medial Superior Frontal Gyrus
	2965	12419.79	0.013	−50 −20 18	R Postcentral
	1074	9651.36	0.029	−9 −73 −9	L Lingual Gyrus
Gyrification Index					
G Carrier E4 Neg > AA E4 Neg	603	3165.66	0.012	−41 −47 37	L Inferior Parietal
	866	2912.02	0.015	−26 −60 47	L Superior Parietal
	155	2580.45	0.019	61 5 14	R Precentral Gyrus
	275	2511.59	0.021	−59 −12 38	L Precentral Gyrus
	78	1633.14	0.048	60 −22 24	R Postcentral Gyrus

Results are listed at a threshold of $p < 0.05$ FWE TFCE corrected, primary peaks within cluster listed in table. Coordinates listed are Montreal Neurological Institute. L; Left, R; Right; Neg; Noncarrier of *ε4* genotype.

the middle temporal cortex, both E4-negative individuals, arguing for a unique *TOMM40*'650 effect on brain structure. Our data fit with previous studies showing the relationship of *TOMM40*'650 with brain volume across the medial temporal, superior temporal, and limbic structure. Several studies using the ADNI dataset have reported associations *TOMM40*'650 with hippocampal volume using whole genome association approaches, both in cross-section and longitudinal atrophy measures[51,55,69]. Another ADNI study used a comprehensive gene and imaging approach and identified a relationship between *TOMM40*'650 and the caudate nucleus[47]. Our findings of '650-related morphological variation were in the temporal cortex, which plays a specific role in language and memory. While we did not test associations between cortical morphometry and cognitive ability on language functions, it is interesting that several studies have identified associations between *TOMM40*'650 and delayed verbal recall ability[1] and decreased language comprehension network strength in females, correlated with increasing age [35].

We investigated the interactive relationship between *TOMM40*'650 G-carriage and sex on aging-related associations of brain structure and plasma biomarkers because of several studies showing sex-specific effects of *TOMM40*'650[35,54]. Li et al. identified an interactive effect of sex with *TOMM40*'650 and language network strength, with the effect specifically in women. Our analysis showed no significant interactions between *TOMM40*'650 and sex on plasma ATN biomarkers. However, in our post-hoc analysis of specific gray matter volumes, there were several brain regions where *TOMM40*'650 G-carrying females had more decreased brain volume with age, namely the middle temporal gyrus and rectus gyrus. GFAP serves as a marker for astrocyte activation and is also related to cognitive health and neurodegenerative disease [36,63]. A smaller study found an association between *TOMM40* poly-T variants (rs10542523) and NfL in CSF [9]. Despite several studies showing a possible relationship between *TOMM40* '650 and plasma and CSF measures of Aβ-42 and Tau [31,59], we did not see a relationship of '650 alleles with plasma Aβ −42/40. This may be due to our sample size, and thus, a more extensive analysis focusing on '650 (outside of the APOE ε4) and Aβ 42/40 in plasma, and, ideally, CSF will be

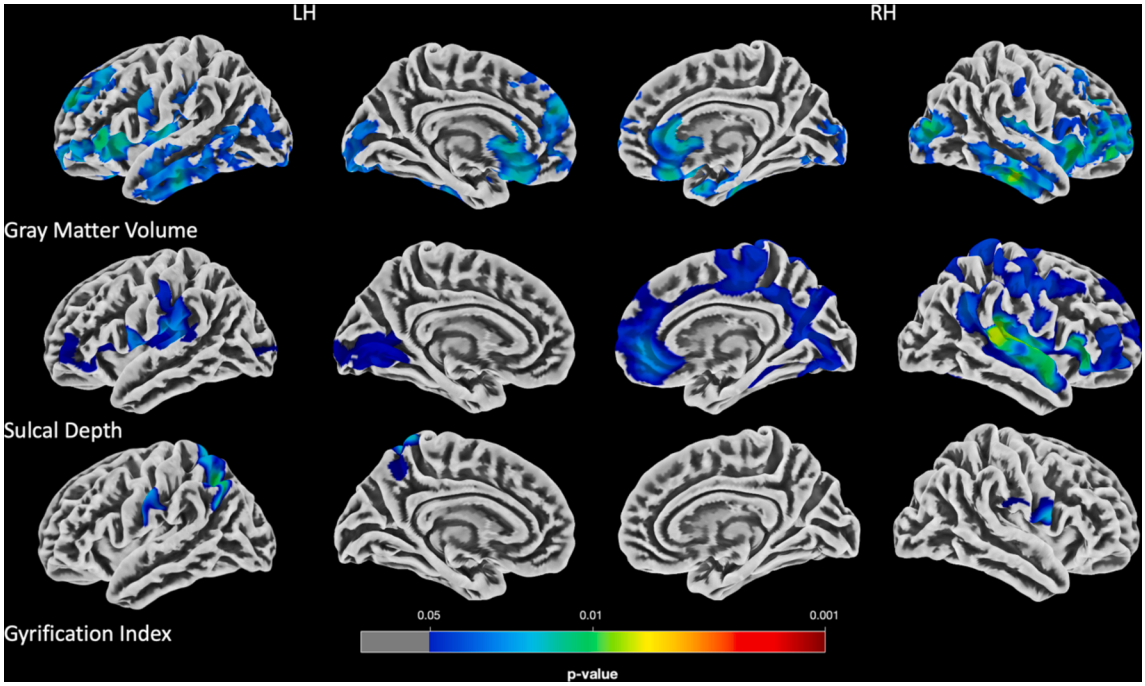

Fig. 3. Clusters showing significantly different cortical morphology in the *TOMM40 '650* G-Carrier group compared to the AA individuals in *APOE* ε*3* individuals only. LH (RH): left (right) hemisphere.

necessary for the future. We did, however, see a relationship between *TOMM40* '650 and plasma tau, in line with Kulminski et al., possibly narrowing the functional implications of TOMM40 genetic variation to neuronal injury and neurodegeneration (associated with tau) over-accumulation of Aβ. While *APOE* most likely contributes to neurodegeneration in aging and AD, there have not been clear associations with *APOE* ε4 and NfL [56,57], and an interplay of nearby genes like *TOMM40* may contribute specifically to structural vulnerability.

TOMM40 may also play a role in other diseases outside of Alzheimer's disease. For instance, McFarquhar et al showed a relationship of *TOMM40*'650 with diagnosis of depression and related changes in brain activation[43]. A recent GWAS study identified SPSs in *TOMM40* and *APOE* associated with dementia with lewy body (DLB) [8]. The presence of the *TOMM40*'523 S allele in *APOE* ε3 individuals has also been shown to impact the rate of cognitive decline in Parkinson's disease and Parkinson's disease dementia[6]. There is growing evidence that *APOE* and *TOMM40* genes work interactively on Chromosome 19 to impact downstream mitochondrial metabolic function in aging [10], possibly explaining the contribution of SNPs like '*650* on overall brain function, aging, and risk for neurodegenerative disease. *TOMM40* and *APOC1* genes modulate the effect of the *APOE* ε4, and this interplay of genes may explain the differing roles of Aβ and Tau in the pathology of AD, as well as the age of onset of AD [31,40]. Our analysis in aging individuals shows that *TOMM40*'650 G allele impacts the brain. However, a larger study on the interacting effects *of TOMM40*'650 G, *APOE*, and *APOC1* will be needed to increase the numbers in the risk G/G group and understand these relationships in the larger context of compound risk genotypes.

Study Limitations

We are limited by the cross-sectional nature of the design of this observational study and cannot infer causality or longitudinal risk based on these results. The KUADRC Clinical cohort is primarily Caucasian and typically shows tight linkage disequilibrium between APOE ε4, and *TOMM40*'650 G alleles, evidenced in this sample. We did, however, test the independent contributions of the *TOMM40*'650 G-allele and *APOE* ε4, albeit with small sample size.

Although work remains to be done to identify appropriate diagnostic cut-off points for the clinical use of biomarkers, [46,52]blood-based biomarkers are moving to the forefront of Alzheimer's disease research. With the continued development of blood biomarkers and efforts to standardize biomarker processing[4,75], it is widely acknowledged that blood biomarkers may provide reliable screening information to aid diagnosis and monitoring of efficacy in a relatively non-invasive and cost-effective manner [2]. NfL is considered to have potential as a prognostic and susceptibility biomarker in both clinical and research settings [28], and both NfL and GFAP predict cognitive decline in a similar manner to neuroimaging analysis. [45].

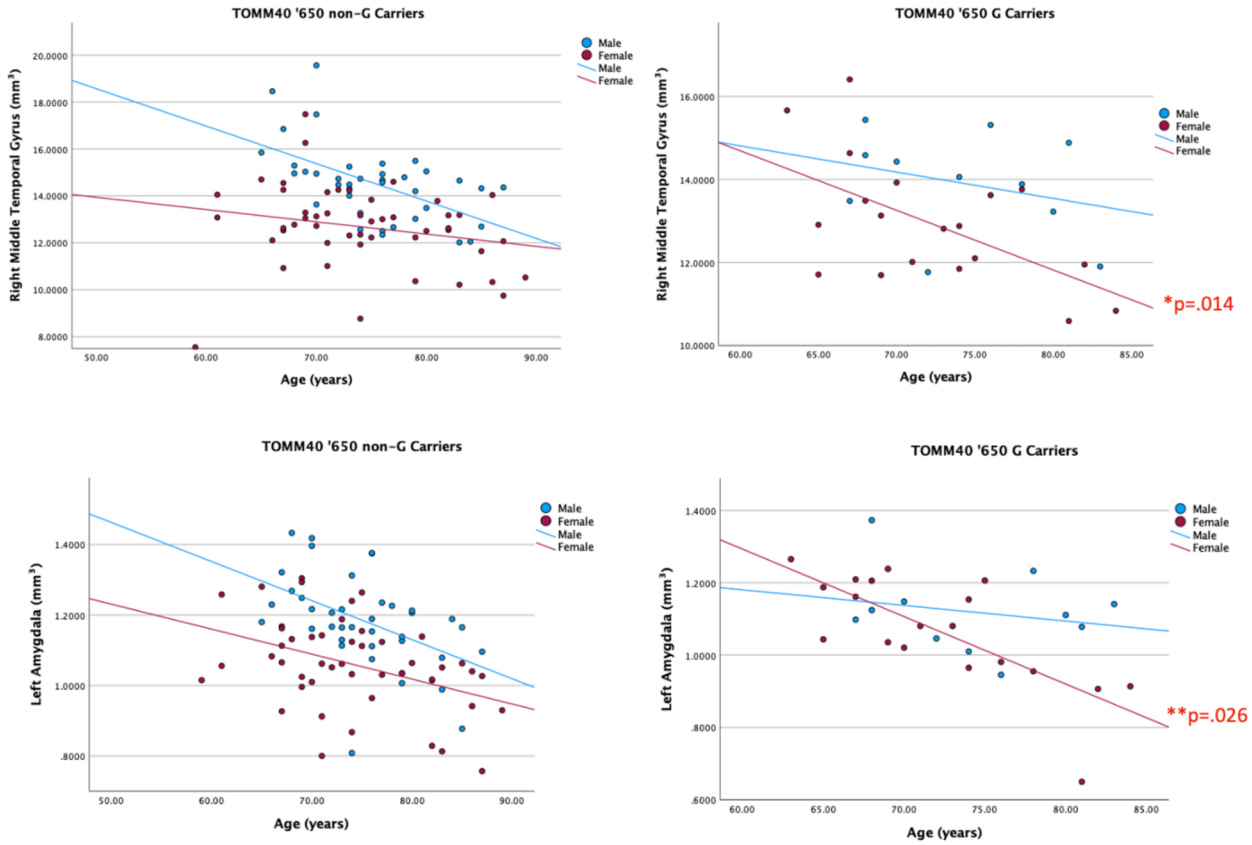

Fig. 4. Regional volume across age differs between sex and TOMM40 '650 G-Carriers. Red and blue circles represent datapoints for women and men, *interaction of '650 x age x sex, **interaction of '650 x sex. The right middle temporal gyrus and the left amygdala were statistically significant results from the interaction analysis and the plots are for viewing purposes.

Table 5
Interactions of TOMM40 '650 G Carriage with age and sex on gray matter volumes.

	Sig	F	Sig	F	Sig	F
	650 x Age		**650 x sex**		**650 x age x sex**	
Right Amygdala	0.272	1.2	0.104	2.695	0.262	1.355
Left Amygdala	0.091	2.915	**0.026**	**5.103**	0.095	2.406
Right Hippocampus	0.772	0.085	0.483	0.068	0.469	0.104
Left Hippocampus	0.224	1.498	0.137	2.24	0.139	2.007
Right Superior Temporal Gyrus	0.139	2.24	0.146	2.14	0.124	2.28
Left Superior Temporal Gyrus	0.19	1.74	0.138	2.24	0.185	1.73
Right Middle Temporal Gyrus	**0.021**	**5.449**	**0.011**	**6.779**	**0.014**	**4.461**
Left Middle Temporal Gyrus	0.139	2.224	0.069	3.386	0.081	2.568
Right Parahippocampal Gyrus	0.549	0.361	0.395	0.731	0.713	0.339
Left Parahippocampal Gyrus	0.273	1.212	0.339	1.63	0.174	0.834
Right Olfactory Cortex	**0.044**	**4.14**	**0.032**	**4.72**	0.061	2.87
Left Olfactory Cortex	0.217	1.54	0.179	1.83	0.261	1.36
Right Rectus Gyrus	0.407	0.694	0.382	0.771	0.124	2.12
Left Rectus Gyrus	0.125	2.39	0.133	2.287	**0.017**	**4.204**

Significant estimates in Bold are $p < 0.05$, controlling for APOE ε4 Haplogroup, age, and sex.

5. Conclusion

Our study is the first to use comprehensive morphological analysis techniques to show varying levels of impact of the *TOMM40*'650 *G* allele on AD-related brain phenotypes. We found that *TOMM40* '650 G-allele was associated with decreased sulcal depth, increased gyrification index and decreased gray matter, and that NfL, pTau181 and GFAP were more associated with age in individuals with a G-allele. Our data suggest that *TOMM40 '650* may be associated with early brain structure variation in temporo-limbic circuits. These findings collectively contribute to the ongoing discourse on how genetic factors such as the *TOMM40* '650 variant may influence brain

structure and function, especially in relation to aging and Alzheimer's disease. This research underscores the complexity of genetic influence on brain integrity. It suggests that the impact of such polymorphisms may vary depending on additional factors like age, sex, and other genetic risk factors.

CRediT authorship contribution statement

Robyn A. Honea: Writing – review & editing, Writing – original draft, Visualization, Supervision, Methodology, Investigation, Funding acquisition, Formal analysis, Data curation, Conceptualization. **Heather Wilkins:** Resources, Methodology, Data curation. **Suzanne L. Hunt:** Writing – review & editing, Validation, Resources, Formal analysis, Data curation. **Paul J. Kueck:** Writing – review & editing, Methodology, Data curation. **Jeffrey M. Burns:** Resources, Project administration, Methodology, Investigation, Funding acquisition. **Russell H. Swerdlow:** Supervision, Resources, Methodology, Data curation, Conceptualization. **Jill K. Morris:** Writing – review & editing, Validation, Supervision, Resources, Project administration, Methodology, Funding acquisition, Data curation.

Declaration of competing interest

The authors declare that they have no known competing financial interests or personal relationships that could have appeared to influence the work reported in this paper.

Acknowledgments

Portions of this work were supported by the following grants: R03AG026374, R21AG029615, R01AG034614, R01AG033673, R01AG062548, R21AG061548, R00AG050490, from the National Institutes on Aging, K23NS058252 from the National Institute on Neurological Disorders and Stroke, and the Alzheimer's Association Park the Cloud Grant. The University of Kansas Alzheimer's Disease Research Center Cohort is supported grant P30AG035982 and P30AG072973 (Cohort). The Hoglund Biomedical Imaging Center is supported by grants C76 HF00201, S10 RR29577, UL1 TR000001. Much of the study data were collected and managed using REDCap electronic data capture tools hosted at University of Kansas Medical Center [23,24]. REDCap (Research Electronic Data Capture) is a secure, web-based software platform designed to support data capture for research studies and is provided for by CTSA Award # UL1TR002366.The authors thank the members of the KU ADRC team for their assistance with data collection and study support, and the participants at the KU ADRC for their generosity of time and spirit, which makes this research possible.

References

[1] Arpawong TE, Pendleton N, Mekli K, McArdle JJ, Gatz M, Armoskus C, et al. Genetic variants specific to aging-related verbal memory: Insights from GWASs in a population-based cohort. PLoS One 2017;12(8). https://doi.org/10.1371/journal.pone.0182448.e0182448.
[2] Arslan B, Zetterberg H, Ashton NJ. Blood-based biomarkers in Alzheimer's disease - moving towards a new era of diagnostics. Clin Chem Lab Med 2024;62(6):1063–9. https://doi.org/10.1515/cclm-2023-1434.
[3] Ashburner, J., 2007. A fast diffeomorphic image registration algorithm. Neuroimage 38(1), 95-113. https://doi.org:S1053-8119(07)00584-8 [pii] 10.1016/j.neuroimage.2007.07.007.
[4] Assfaw AD, Schindler SE, Morris JC. Advances in blood biomarkers for Alzheimer disease (AD): A review. Kaohsiung J Med Sci 2024. https://doi.org/10.1002/kjm2.12870.
[5] Bachmann T, Schroeter ML, Chen K, Reiman EM, Weise CM, Neuroimaging AD, et al. Longitudinal changes in surface based brain morphometry measures in amnestic mild cognitive impairment and Alzheimer's Disease. NeuroImage Clinical 2023;38:103371. https://doi.org/10.1016/j.nicl.2023.103371.
[6] Bakeberg MC, Gorecki AM, Pfaff AL, Hoes ME, Koks S, Akkari PA, et al. TOMM40 '523' poly-T repeat length is a determinant of longitudinal cognitive decline in Parkinson's disease. NPJ Parkinsons Dis 2021;7(1):56. https://doi.org/10.1038/s41531-021-00200-y.
[7] Beach TG, Monsell SE, Phillips LE, Kukull W. Accuracy of the clinical diagnosis of Alzheimer disease at National Institute on Aging Alzheimer Disease Centers, 2005–2010. J Neuropathol Exp Neurol 2012;71(4):266–73. https://doi.org/10.1097/NEN.0b013e31824b211b.
[8] Bras J, Guerreiro R, Darwent L, Parkkinen L, Ansorge O, Escott-Price V, et al. Genetic analysis implicates APOE, SNCA and suggests lysosomal dysfunction in the etiology of dementia with Lewy bodies. Hum Mol Genet 2014;23(23):6139–46. https://doi.org/10.1093/hmg/ddu334.
[9] Bruno D, Pomara N, Nierenberg J, Ritchie JC, Lutz MW, Zetterberg H, et al. Levels of cerebrospinal fluid neurofilament light protein in healthy elderly vary as a function of TOMM40 variants. Exp Gerontol 2012;47(5):347–52. https://doi.org/10.1016/j.exger.2011.09.008.
[10] Caselli RJ, Dueck AC, Huentelman MJ, Lutz MW, Saunders AM, Reiman EM, et al. Longitudinal modeling of cognitive aging and the TOMM40 effect. Alzheimers Dement 2012;8(6):490–5. https://doi.org/10.1016/j.jalz.2011.11.006.
[11] Chen S, Sarasua SM, Davis NJ, DeLuca JM, Boccuto L, Thielke SM, et al. TOMM40 genetic variants associated with healthy aging and longevity: a systematic review. BMC Geriatr 2022;22(1):667. https://doi.org/10.1186/s12877-022-03337-4.
[12] Chiba-Falek O, Gottschalk WK, Lutz MW. The effects of the TOMM40 poly-T alleles on Alzheimer's disease phenotypes. Alzheimers Dement 2018;14(5):692–8. https://doi.org/10.1016/j.jalz.2018.01.015.
[13] Choi M, Youn H, Kim D, Lee S, Suh S, Seong JK, et al. Comparison of neurodegenerative types using different brain MRI analysis metrics in older adults with normal cognition, mild cognitive impairment, and Alzheimer's dementia. PLoS One 2019;14(8). https://doi.org/10.1371/journal.pone.0220739.e0220739.
[14] Deelen J, Beekman M, Uh HW, Broer L, Ayers KL, Tan Q, et al. Genome-wide association meta-analysis of human longevity identifies a novel locus conferring survival beyond 90 years of age. Hum Mol Genet 2014;23(16):4420–32. https://doi.org/10.1093/hmg/ddu139.
[15] Desikan RS, Segonne F, Fischl B, Quinn BT, Dickerson BC, Blacker D, et al. An automated labeling system for subdividing the human cerebral cortex on MRI scans into gyral based regions of interest. Neuroimage 2006;31(3):968–80. https://doi.org/10.1016/j.neuroimage.2006.01.021.
[16] Du AT, Schuff N, Kramer JH, Rosen HJ, Gorno-Tempini ML, Rankin K, et al. Different regional patterns of cortical thinning in Alzheimer's disease and frontotemporal dementia. Brain 2007;130(Pt 4):1159–66. https://doi.org/10.1093/brain/awm016.
[17] Eklund A, Nichols TE, Knutsson H. Cluster failure: Why fMRI inferences for spatial extent have inflated false-positive rates. Proc Natl Acad Sci U S A 2016;113(28):7900–5. https://doi.org/10.1073/pnas.1602413113.
[18] Fortney K, Dobriban E, Garagnani P, Pirazzini C, Monti D, Mari D, et al. Genome-Wide Scan Informed by Age-Related Disease Identifies Loci for Exceptional Human Longevity. PLoS Genet 2015;11(12). https://doi.org/10.1371/journal.pgen.1005728.e1005728.
[19] Good CD, Ashburner J, Frackowiak RS. Computational neuroanatomy: new perspectives for neuroradiology. Rev Neurol (Paris) 2001;157(8–9 Pt 1):797–806.

[20] Gottschalk WK, Lutz MW, He YT, Saunders AM, Burns DK, Roses AD, et al. The Broad Impact of TOM40 on Neurodegenerative Diseases in Aging. J Parkinsons Dis Alzheimers Dis 2014;1(1). https://doi.org/10.13188/2376-922X.1000003.

[21] Green ZD, Kueck PJ, John CS, Burns JM, Morris JK. Blood Biomarkers Discriminate Cerebral Amyloid Status and Cognitive Diagnosis when Collected with ACD-A Anticoagulant. Curr Alzheimer Res 2023;20(8):557–66. https://doi.org/10.2174/0115672050271523231111192725.

[22] Gui W, Qiu C, Shao Q, Li J. Associations of Vascular Risk Factors, APOE and TOMM40 Polymorphisms With Cognitive Function in Dementia-Free Chinese Older Adults: A Community-Based Study. Front Psychiatry 2021;12:617773. https://doi.org/10.3389/fpsyt.2021.617773.

[23] Harris PA, Taylor R, Minor BL, Elliott V, Fernandez M, O'Neal L, McLeod L, Delacqua G, Delacqua F, Kirby J, Duda SN, Consortium RE. The REDCap consortium: Building an international community of software platform partners. J Biomed Inform 2019;95:103208. https://doi.org/10.1016/j.jbi.2019.103208.

[24] Harris, P.A., Taylor, R., Thielke, R., Payne, J., Gonzalez, N., Conde, J.G., 2009. Research electronic data capture (REDCap)–a metadata-driven methodology and workflow process for providing translational research informatics support. J Biomed Inform 42(2), 377-381. https://doi.org:S1532-0464(08)00122-6 [pii]. 10.1016/j.jbi.2008.08.010.

[25] Honea RA, Hunt S, Lepping RJ, Vidoni ED, Morris JK, Watts A, et al. Alzheimer's disease cortical morphological phenotypes are associated with TOMM40'523-APOE haplotypes. Neurobiol Aging 2023;132:131–44. https://doi.org/10.1016/j.neurobiolaging.2023.09.001.

[26] Honea, R.A., Swerdlow, R.H., Vidoni, E.D., Goodwin, J., Burns, J.M., Reduced gray matter volume in normal adults with a maternal family history of Alzheimer disease. Neurology 74(2), 113-120. https://doi.org:74/2/113 [pii]. 10.1212/WNL.0b013e3181c918cb.

[27] Im K, Lee JM, Seo SW, Hyung Kim S, Kim SI, Na DL. Sulcal morphology changes and their relationship with cortical thickness and gyral white matter volume in mild cognitive impairment and Alzheimer's disease. Neuroimage 2008;43(1):103–13. https://doi.org/10.1016/j.neuroimage.2008.07.016.

[28] Jung Y, Damoiseaux JS. The potential of blood neurofilament light as a marker of neurodegeneration for Alzheimer's disease. Brain 2024;147(1):12–25. https://doi.org/10.1093/brain/awad267.

[29] Kalin AM, Park MT, Chakravarty MM, Lerch JP, Michels L, Schroeder C, et al. Subcortical Shape Changes, Hippocampal Atrophy and Cortical Thinning in Future Alzheimer's Disease Patients. Front Aging Neurosci 2017;9:38. https://doi.org/10.3389/fnagi.2017.00038.

[30] King RD, Brown B, Hwang M, Jeon T, George AT, Neuroimaging AD, et al. Fractal dimension analysis of the cortical ribbon in mild Alzheimer's disease. Neuroimage 2010;53(2):471–9. https://doi.org/10.1016/j.neuroimage.2010.06.050.

[31] Kulminski AM, Jain-Washburn E, Loiko E, Loika Y, Feng F, Culminskaya I, et al. Associations of the APOE epsilon2 and epsilon4 alleles and polygenic profiles comprising APOE-TOMM40-APOC1 variants with Alzheimer's disease biomarkers. Aging (Albany NY) 2022;14(24):9782–804. https://doi.org/10.18632/aging.204384.

[32] Kulminski, A.M., Loika, Y., Culminskaya, I., Huang, J., Arbeev, K.G., Bagley, O., Feitosa, M.F., Zmuda, J.M., Christensen, K., Yashin, A.I., Long Life Family Study Research, G., 2019. Independent associations of TOMM40 and APOE variants with body mass index. Aging Cell 18(1), e12869. https://doi.org:10.1111/acel.12869.

[33] Kulminski AM, Philipp I, Shu L, Culminskaya I. Definitive roles of TOMM40-APOE-APOC1 variants in the Alzheimer's risk. Neurobiol Aging 2022;110:122–31. https://doi.org/10.1016/j.neurobiolaging.2021.09.009.

[34] Lamparello AJ, Namas RA, Schimunek L, Cohen M, El-Dehaibi F, Yin J, et al. An Aging-Related Single-Nucleotide Polymorphism is Associated With Altered Clinical Outcomes and Distinct Inflammatory Profiles in Aged Blunt Trauma Patients. Shock 2020;53(2):146–55. https://doi.org/10.1097/SHK.0000000000001411.

[35] Li T, Pappas C, Le ST, Wang Q, Klinedinst BS, Larsen BA, et al. APOE, TOMM40, and sex interactions on neural network connectivity. Neurobiol Aging 2022;109:158–65. https://doi.org/10.1016/j.neurobiolaging.2021.09.020.

[36] Liddelow SA, Barres BA. Reactive Astrocytes: Production, Function, and Therapeutic Potential. Immunity 2017;46(6):957–67. https://doi.org/10.1016/j.immuni.2017.06.006.

[37] Liu H, Liu T, Jiang J, Cheng J, Liu Y, Li D, et al. Differential longitudinal changes in structural complexity and volumetric measures in community-dwelling older individuals. Neurobiol Aging 2020;91:26–35. https://doi.org/10.1016/j.neurobiolaging.2020.02.023.

[38] Liu X, Song Z, Li Y, Yao Y, Fang M, Bai C, et al. Integrated genetic analyses revealed novel human longevity loci and reduced risks of multiple diseases in a cohort study of 15,651 Chinese individuals. Aging Cell 2021;20(3). https://doi.org/10.1111/acel.13323.e13323.

[39] Lu F, Guan H, Gong B, Liu X, Zhu R, Wang Y, et al. Genetic variants in PVRL2-TOMM40-APOE region are associated with human longevity in a Han Chinese population. PLoS One 2014;9(6). https://doi.org/10.1371/journal.pone.0099580.e99580.

[40] Lutz MW, Crenshaw DG, Saunders AM, Roses AD. Genetic variation at a single locus and age of onset for Alzheimer's disease. Alzheimers Dement 2010;6(2):125–31. https://doi.org/10.1016/j.jalz.2010.01.011.

[41] Lyall DM, Royle NA, Harris SE, Bastin ME, Maniega SM, Murray C, et al. Alzheimer's disease susceptibility genes APOE and TOMM40, and hippocampal volumes in the Lothian birth cohort 1936. PLoS One 2013;8(11). https://doi.org/10.1371/journal.pone.0080513.e80513.

[42] Marzi C, Giannelli M, Tessa C, Mascalchi M, Diciotti S. Toward a more reliable characterization of fractal properties of the cerebral cortex of healthy subjects during the lifespan. Sci Rep 2020;10(1):16957. https://doi.org/10.1038/s41598-020-73961-w.

[43] McFarquhar M, Elliott R, McKie S, Thomas E, Downey D, Mekli K, et al. TOMM40 rs2075650 may represent a new candidate gene for vulnerability to major depressive disorder. Neuropsychopharmacology : official publication of the American College of Neuropsychopharmacology 2014;39(7):1743–53. https://doi.org/10.1038/npp.2014.22.

[44] McKhann GM, Knopman DS, Chertkow H, Hyman BT, Jack Jr CR, Kawas CH, et al. The diagnosis of dementia due to Alzheimer's disease: recommendations from the National Institute on Aging-Alzheimer's Association workgroups on diagnostic guidelines for Alzheimer's disease. Alzheimers Dement 2011;7(3):263–9. https://doi.org/10.1016/j.jalz.2011.03.005.

[45] Mendes AJ, Ribaldi F, Lathuiliere A, Ashton NJ, Zetterberg H, Abramowicz M, et al. Comparison of plasma and neuroimaging biomarkers to predict cognitive decline in non-demented memory clinic patients. Alzheimers Res Ther 2024;16(1):110. https://doi.org/10.1186/s13195-024-01478-9.

[46] Mielke MM, Fowler NR. Alzheimer disease blood biomarkers: considerations for population-level use. Nat Rev Neurol 2024. https://doi.org/10.1038/s41582-024-00989-1.

[47] Moon SW, Dinov ID, Kim J, Zamanyan A, Hobel S, Thompson PM, et al. Structural Neuroimaging Genetics Interactions in Alzheimer's Disease. J Alzheimers Dis 2015;48(4):1051–63. https://doi.org/10.3233/JAD-150335.

[48] Morris JC. The Clinical Dementia Rating (CDR): current version and scoring rules. Neurology 1993;43(11):2412b–b2414.

[49] A. Omoumi A. Fok T. Greenwood A.D. Sadovnick H.H. Feldman G.Y. Hsiung Evaluation of late-onset Alzheimer disease genetic susceptibility risks in a Canadian population Neurobiology of aging 35 4 2014 936 e935–912 10.1016/j.neurobiolaging.2013.09.025.

[50] Ortega-Rojas J, Arboleda-Bustos CE, Guerrero E, Neira J, Arboleda H. Genetic Variants and Haplotypes of TOMM40, APOE, and APOC1 are Related to the Age of Onset of Late-onset Alzheimer Disease in a Colombian Population. Alzheimer Dis Assoc Disord 2022;36(1):29–35. https://doi.org/10.1097/WAD.0000000000000477.

[51] Potkin SG, Guffanti G, Lakatos A, Turner JA, Kruggel F, Fallon JH, et al. Hippocampal atrophy as a quantitative trait in a genome-wide association study identifying novel susceptibility genes for Alzheimer's disease. PLoS One 2009;4(8). https://doi.org/10.1371/journal.pone.0006501.e6501.

[52] Schindler SE, Galasko D, Pereira AC, Rabinovici GD, Salloway S, Suarez-Calvet M, et al. Acceptable performance of blood biomarker tests of amyloid pathology - recommendations from the Global CEO Initiative on Alzheimer's Disease. Nat Rev Neurol 2024;20(7):426–39. https://doi.org/10.1038/s41582-024-00977-5.

[53] Sebastiani P, Solovieff N, Dewan AT, Walsh KM, Puca A, Hartley SW, et al. Genetic signatures of exceptional longevity in humans. PLoS One 2012;7(1). https://doi.org/10.1371/journal.pone.0029848.e29848.

[54] Shadyab AH, Kooperberg C, Reiner AP, Jain S, Manson JE, Hohensee C, et al. Replication of Genome-Wide Association Study Findings of Longevity in White, African American, and Hispanic Women: The Women's Health Initiative. J Gerontol A Biol Sci Med Sci 2017;72(10):1401–6. https://doi.org/10.1093/gerona/glw198.

[55] Shen L, Kim S, Risacher SL, Nho K, Swaminathan S, West JD, et al. Whole genome association study of brain-wide imaging phenotypes for identifying quantitative trait loci in MCI and AD: A study of the ADNI cohort. Neuroimage 2010;53(3):1051–63. https://doi.org/10.1016/j.neuroimage.2010.01.042.

[56] Sjogren M, Blomberg M, Jonsson M, Wahlund LO, Edman A, Lind K, et al. Neurofilament protein in cerebrospinal fluid: a marker of white matter changes. J Neurosci Res 2001;66(3):510–6. https://doi.org/10.1002/jnr.1242.
[57] Sjogren M, Rosengren L, Minthon L, Davidsson P, Blennow K, Wallin A. Cytoskeleton proteins in CSF distinguish frontotemporal dementia from AD. Neurology 2000;54(10):1960–4. https://doi.org/10.1212/wnl.54.10.1960.
[58] Smith SM, Nichols TE. Threshold-free cluster enhancement: addressing problems of smoothing, threshold dependence and localisation in cluster inference. Neuroimage 2009;44(1):83–98. https://doi.org/10.1016/j.neuroimage.2008.03.061.
[59] Souza MB, Araujo GS, Costa IG, Oliveira JR, Neuroimaging AD, I.. Combined Genome-Wide CSF Abeta-42's Associations and Simple Network Properties Highlight New Risk Factors for Alzheimer's Disease. Journal of molecular neuroscience : MN 2016;58(1):120–8. https://doi.org/10.1007/s12031-015-0667-6.
[60] Swerdlow RH. Alzheimer's disease pathologic cascades: who comes first, what drives what. Neurotox Res 2012;22(3):182–94. https://doi.org/10.1007/s12640-011-9272-9.
[61] Torres GG, Dose J, Hasenbein TP, Nygaard M, Krause-Kyora B, Mengel-From J, et al. Long-Lived Individuals Show a Lower Burden of Variants Predisposing to Age-Related Diseases and a Higher Polygenic Longevity Score. Int J Mol Sci 2022;23(18). https://doi.org/10.3390/ijms231810949.
[62] Varathan P, Gorijala P, Jacobson T, Chasioti D, Nho K, Risacher SL, et al. Integrative analysis of eQTL and GWAS summary statistics reveals transcriptomic alteration in Alzheimer brains. BMC Med Genomics 2022;15(Suppl 2):93. https://doi.org/10.1186/s12920-022-01245-5.
[63] Verberk IMW, Thijssen E, Koelewijn J, Mauroo K, Vanbrabant J, de Wilde A, et al. Combination of plasma amyloid beta((1–42/1-40)) and glial fibrillary acidic protein strongly associates with cerebral amyloid pathology. Alzheimers Res Ther 2020;12(1):118. https://doi.org/10.1186/s13195-020-00682-7.
[64] Vidoni ED, Van Sciver A, Johnson DK, He J, Honea R, Haines B, et al. A community-based approach to trials of aerobic exercise in aging and Alzheimer's disease. Contemp Clin Trials 2012;33(6):1105–16. https://doi.org/10.1016/j.cct.2012.08.002.
[65] Watts A, Wilkins HM, Michaelis E, Swerdlow RH. TOMM40 '523 Associations with Baseline and Longitudinal Cognition in APOE varepsilon3 Homozygotes. J Alzheimers Dis 2019;70(4):1059–68. https://doi.org/10.3233/JAD-190293.
[66] Weintraub S, Salmon D, Mercaldo N, Ferris S, Graff-Radford NR, Chui H, et al. The Alzheimer's Disease Centers' Uniform Data Set (UDS): the neuropsychologic test battery. Alzheimer Dis Assoc Disord 2009;23(2):91–101. https://doi.org/10.1097/WAD.0b013e318191c7dd.
[67] Wilkins HM, Koppel SJ, Bothwell R, Mahnken J, Burns JM, Swerdlow RH. Platelet cytochrome oxidase and citrate synthase activities in APOE epsilon4 carrier and non-carrier Alzheimer's disease patients. Redox Biol 2017;12:828–32. https://doi.org/10.1016/j.redox.2017.04.010.
[68] Xiong C, Roe CM, Buckles V, Fagan A, Holtzman D, Balota D, et al. Role of family history for Alzheimer biomarker abnormalities in the adult children study. Arch Neurol 2011;68(10):1313–9. https://doi.org/10.1001/archneurol.2011.208.
[69] Xu Z, Shen X, Pan W, Neuroimaging AD, I.. Longitudinal analysis is more powerful than cross-sectional analysis in detecting genetic association with neuroimaging phenotypes. PLoS One 2014;9(8). https://doi.org/10.1371/journal.pone.0102312.e102312.
[70] Yashin AI, Arbeev KG, Wu D, Arbeeva LS, Bagley O, Stallard E, et al. Genetics of Human Longevity From Incomplete Data: New Findings From the Long Life Family Study. J Gerontol A Biol Sci Med Sci 2018;73(11):1472–81. https://doi.org/10.1093/gerona/gly057.
[71] Yashin AI, Fang F, Kovtun M, Wu D, Duan M, Arbeev K, et al. Hidden heterogeneity in Alzheimer's disease: Insights from genetic association studies and other analyses. Exp Gerontol 2018;107:148–60. https://doi.org/10.1016/j.exger.2017.10.020.
[72] Yotter RA, Nenadic I, Ziegler G, Thompson PM, Gaser C. Local cortical surface complexity maps from spherical harmonic reconstructions. Neuroimage 2011;56(3):961–73. https://doi.org/10.1016/j.neuroimage.2011.02.007.
[73] Yotter RA, Thompson PM, Gaser C. Algorithms to improve the reparameterization of spherical mappings of brain surface meshes. Journal of neuroimaging : official journal of the American Society of Neuroimaging 2011;21(2):e134–47. https://doi.org/10.1111/j.1552-6569.2010.00484.x.
[74] Yun HJ, Im K, Jin-Ju Y, Yoon U, Lee JM. Automated sulcal depth measurement on cortical surface reflecting geometrical properties of sulci. PLoS One 2013;8(2). https://doi.org/10.1371/journal.pone.0055977.e55977.
[75] Zeng X, Chen Y, Sehrawat A, Lee J, Lafferty TK, Kofler J, et al. Alzheimer blood biomarkers: practical guidelines for study design, sample collection, processing, biobanking, measurement and result reporting. Mol Neurodegener 2024;19(1):40. https://doi.org/10.1186/s13024-024-00711-1.